The 18 O-signal transfer from water vapour to leaf water and assimilates varies among plant species and growth forms

Marco M Lehmann, Gregory R Goldsmith, Cathleen Mirande-ney, Rosemarie B Weigt, Leonie Schönbeck, Ansgar Kahmen, Arthur Gessler, Rolf T W Siegwolf, Matthias Saurer

HAL Id: hal-04901766

https://hal.inrae.fr/hal-04901766v1

Submitted on 20 Jan 2025

ORIGINAL ARTICLE

WILEY — Plant, Cell & Environment

The ^{18}O-signal transfer from water vapour to leaf water and assimilates varies among plant species and growth forms

Marco M. Lehmann[1] | Gregory R. Goldsmith[2] | Cathleen Mirande-Ney[3] | Rosemarie B. Weigt[1] | Leonie Schönbeck[1] | Ansgar Kahmen[4] | Arthur Gessler[1] | Rolf T.W. Siegwolf[1] | Matthias Saurer[1]

[1] Forest Dynamics, Swiss Federal Institute for Forest, Snow and Landscape Research (WSL), Birmensdorf 8903, Switzerland

[2] Schmid College of Science and Technology, Chapman University, Orange, CA 92866

[3] CIRAD, UPR Systèmes de Pérennes, Montpellier 34398, France

[4] Department of Environmental Sciences-Botany, University of Basel, Basel 4056, Switzerland

Correspondence
Marco M. Lehmann, Swiss Federal Institute for Forest, Snow and Landscape Research (WSL), Zuercherstrasse 111, 8903 Birmensdorf, Switzerland.
Email: marco.lehmann@alumni.ethz.ch

Funding information
Swiss National Science Foundation, Grant/Award Number: 200020_166162

Abstract

The ^{18}O signature of atmospheric water vapour ($\delta^{18}O_V$) is known to be transferred via leaf water to assimilates. It remains, however, unclear how the ^{18}O-signal transfer differs among plant species and growth forms. We performed a 9-hr greenhouse fog experiment (relative humidity $\geq$ 98%) with ^{18}O-depleted water vapour (−106.7‰) on 140 plant species of eight different growth forms during daytime. We quantified the ^{18}O-signal transfer by calculating the mean residence time of O in leaf water (MRT_{LW}) and sugars (MRT_{Sugars}) and related it to leaf traits and physiological drivers. MRT_{LW} increased with leaf succulence and thickness, varying between 1.4 and 10.8 hr. MRT_{Sugars} was shorter in C_3 and C_4 plants than in crassulacean acid metabolism (CAM) plants and highly variable among species and growth forms; MRT_{Sugars} was shortest for grasses and aquatic plants, intermediate for broadleaf trees, shrubs, and herbs, and longest for conifers, epiphytes, and succulents. Sucrose was more sensitive to $\delta^{18}O_V$ variations than other assimilates. Our comprehensive study shows that plant species and growth forms vary strongly in their sensitivity to $\delta^{18}O_V$ variations, which is important for the interpretation of $\delta^{18}O$ values in plant organic material and compounds and thus for the reconstruction of climatic conditions and plant functional responses.

KEYWORDS

carbohydrates, clouds, compound-specific isotope analysis (CSIA), fog, foliar water uptake, leaf wetting, precipitation, rain

1 | INTRODUCTION

The oxygen isotopic signature ($\delta^{18}O$) of photosynthetic assimilates (e.g., sugars) and cellulose holds valuable information about plant functional responses to environmental drivers and is therefore widely applied in ecophysiological and dendrochronological researches (Gessler et al., 2014; Helliker & Ehleringer, 2002a; Roden, Lin, & Ehleringer, 2000; Sternberg et al., 2009). The $\delta^{18}O$ composition of plant material is strongly related to leaf water composition ($\delta^{18}O_{LW}$), which is mainly determined by leaf evaporative conditions (Cernusak et al., 2016; Kahmen et al., 2011) and two isotopic sources: (a) $\delta^{18}O$ of source water

($\delta^{18}O_S$) that is taken up by plants from the soil and transported to the leaves via transpiration (Cernusak et al., 2016; Dawson, Mambelli, Plamboeck, Templer, & Tu, 2002) and (b) $\delta^{18}O$ of atmospheric water vapour ($\delta^{18}O_V$) via a bidirectional exchange of water molecules between the leaf and the atmosphere (Goldsmith, Lehmann, Cernusak, Arend, & Siegwolf, 2017; Kim & Lee, 2011). In studies employing $\delta^{18}O$ composition of plant material, $\delta^{18}O_V$ is often assumed to be in equilibrium with $\delta^{18}O_S$, although evidence for this assumption is scarce (Brinkmann et al., 2018; Saurer, Kirdyanov, Prokushkin, Rinne, & Siegwolf, 2016).

However, recent studies demonstrate strong daily and seasonal variations in $\delta^{18}O_V$ on the basis of local, regional, and global

hydrological processes that affect atmospheric weather conditions (Huang & Wen, 2014; Lee, Smith, & Williams, 2006; Tremoy et al., 2012; Yu, Tian, Ma, Xu, & Qu, 2015). This causes $\delta^{18}O_V$ to often be decoupled from $\delta^{18}O_S$ (Bögelein, Thomas, & Kahmen, 2017; Lai et al., 2008). As a consequence, $\delta^{18}O_V$ and $\delta^{18}O_S$ do not covary in their influence on $\delta^{18}O_{LW}$, and disentangling the relative importance of these two water sources on $\delta^{18}O_{LW}$ and thus on $\delta^{18}O$ of plant material is therefore critical (Helliker, 2014; Helliker & Griffiths, 2007; Roden & Ehleringer, 1999). It is currently unclear which leaf functional traits influence uptake and incorporation of the temporal variations in $\delta^{18}O_V$ into the $\delta^{18}O$ values of leaf water and assimilates (Kim & Lee, 2011; Lehmann et al., 2018; Roden & Ehleringer, 1999). A general survey of plant species of different growth forms covering a broad range of functional traits may therefore allow the identification of important drivers of ^{18}O-signal transfer processes and improve the climatic and physiological interpretation of $\delta^{18}O$ signals in plant organic material and compounds, such as the $\delta^{18}O$ of leaf and tree-ring cellulose (Helliker, 2014; Helliker & Griffiths, 2007; Roden & Ehleringer, 1999) or $\delta^{18}O$ of levoglucosan (Blees et al., 2017).

Isotopic composition of leaf water can be modelled, provided that $\delta^{18}O$ values of both water sources are known (Craig & Gordon, 1965; Dongmann, Nurnberg, Forstel, & Wagener, 1974; Flanagan, Comstock, & Ehleringer, 1991).

$$\delta^{18}O_{LW} = \delta^{18}O_S + \varepsilon_{eq} + \varepsilon_k + \left(\delta^{18}O_V - \varepsilon_k - \delta^{18}O_S\right) \times e_a/e_i, \quad (1)$$

where ε_{eq} and ε_k are equilibrium and kinetic fractionation factors, respectively, and e_a/e_i is the ratio of the partial pressure of water vapour outside and inside the leaf. Importantly, the influence of $\delta^{18}O_V$ on $\delta^{18}O_{LW}$ increases as a function of e_a/e_i and is strongest when the atmosphere is completely saturated with water vapour (Helliker, 2014). High humidity conditions cause the stomata to open because transpirational water loss is strongly reduced (i.e., low vapour pressure deficit). This leads to unity between the ratio of the partial pressure of water vapour outside relative to inside the leaf (e_a/e_i = 1). Equation (1) can thus be simplified to

$$\delta^{18}O_{LW} = \delta^{18}O_V + \varepsilon_{eq}. \quad (2)$$

Thus, $\delta^{18}O_V$ variation is particularly important under high humidity conditions. Such conditions are often found in tropical and subtropical forests, where ~50% of days can be very humid (>0.1 mm precipitation), closely followed by temperate and boreal forests (Dawson & Goldsmith, 2018). Further, specific precipitation events such as mist, dew, or fog can lead to high humidity and thus $\delta^{18}O_V$ variation can also be important for plants in many coastal, desert, or montane regions. One means of evaluating the ^{18}O-signal transfer within an individual plant is to calculate the mean residence time of O in leaf water (MRT_{LW}) and assimilates on the basis of the isotope response after a step change in $\delta^{18}O_V$ during a high humidity period. A shorter MRT indicates a faster ^{18}O-signal transfer, which is consistent with changes in the pool size and in the flux going through that pool (or both; Epron et al., 2012). Therefore, MRT values likely depend on leaf

anatomical and morphological properties that can widely differ among plant growth forms (Cernusak, Mejia-Chang, Winter, & Griffiths, 2008; Lai et al., 2008; Liang et al., 2018). Stomata are the primary entry point for $\delta^{18}O_V$ and thus differences in stomata pore size and density may influence the uptake of the atmospheric signal into the leaf water pool (Berry, Emery, Gotsch, & Goldsmith, 2018). In addition, photosynthetic modes (PM; i.e., C_3, C_4, and crassulacean acid metabolism [CAM]) that influence the timing of stomatal opening and leaf water content may also affect MRT_{LW} values and thus the sensitivity of a plant species to $\delta^{18}O_V$ variations (Cernusak et al., 2008; Dubbert, Kübert, & Werner, 2017; Liang et al., 2018). However, studies focusing on the influence of leaf functional traits on the equilibration between $\delta^{18}O_V$ and $\delta^{18}O_{LW}$ and thus MRT_{LW} are scarce (Kim & Lee, 2011; Lai et al., 2008; Roden & Ehleringer, 1999).

Our understanding on how $\delta^{18}O_V$ signals are transferred to $\delta^{18}O$ of plant organic matter and assimilates is even more limited. Research to date has demonstrated that variation in $\delta^{18}O_{LW}$ induced by step changes in $\delta^{18}O_V$ can be incorporated into $\delta^{18}O$ of plant organic matter, and the incorporation may differ among different sugar compounds (Lehmann et al., 2018; Studer, Siegwolf, Leuenberger, & Abiven, 2015). However, it remains unclear if the observed compound-specific pattern, with some compounds being more sensitive to water vapour-induced $\delta^{18}O_{LW}$ variations than others, can be generalized among species and growth forms. Furthermore, the ^{18}O-signal transfer from leaf water to assimilates is known to depend on photosynthetic rates (Lehmann et al., 2018), PM (Helliker & Ehleringer, 2002b), and the turnover of leaf carbohydrate pools (Song, Farquhar, Gessler, & Barbour, 2014). Some studies observed that high humidity conditions such as fog or leaf wetting, that is, when the relevance of $\delta^{18}O_V$ variation is highest, can positively or negatively affect the photosynthetic rates of various species from different biomes (Aparecido, Miller, Cahill, & Moore, 2017; Berry & Smith, 2014; Dawson & Goldsmith, 2018; Eller, Lima, & Oliveira, 2013). We therefore assume that the MRT of O in assimilates will vary strongly among species and growth forms, but this has not yet been quantified.

To provide a more mechanistic understanding of the ^{18}O-signal transfer from water vapour to leaf water and assimilates, we conducted a multispecies ^{18}O-fog experiment and tested (a) how much the ^{18}O-signal transfer differs among plant species and growth forms; (b) whether anatomical (e.g., stomatal density and size), morphological (e.g., leaf thickness and succulence) leaf traits, physiological processes (e.g., leaf gas exchange), leaf sugar pool sizes, and PM (determined via $\delta^{13}C$ values) influence the MRT of O in leaf water and assimilates; as well as (c) identified the assimilates most sensitive to water vapour induced $\delta^{18}O_{LW}$ variations by compound-specific isotope analysis.

2 | MATERIAL AND METHODS

2.1 | Plant material and experimental procedure

We surveyed 140 plant species from eight different growth forms (Table S1), including aquatics (i.e., plants growing in water-covered

sediments or very moist soils with leaves above the water table; $n = 6$ spp.), coniferous trees ($n = 10$ spp.), epiphytes (i.e., nonparasitic plants but growing on other plants; for the experiment, however, all epiphytes were kept on a string above the ground without contact to another plant; generally succulent and CAM; $n = 11$ spp.), grasses ($n = 12$ spp.), herbs ($n = 28$ spp.), succulents (i.e., succulent plants growing on soil, generally CAM; $n = 19$ spp.), broadleaf shrubs ($n = 30$ spp.), and broadleaf trees ($n = 24$ spp.). Plants were obtained from the Botanical Garden of the University of Basel, the garden of the Swiss Federal Institute WSL, and a commercial grower (Hauenstein-Rafz, Zurich, CH). The plant species originate from different ecosystems (e.g., temperate and tropical forests, deserts, and freshwater lakes) and are thus expected to show a high variability in leaf functional traits, leaf gas exchange, PM, and turnover times in water and assimilate pools. Plants were generally potted in standard potting soil, except for epiphytes and some aquatic plants. Plant height/length varied from 4 to 201 cm, with annual plants being fully developed and photosynthetically active at sampling date.

All plants were transferred to a greenhouse at WSL and acclimatized for 4 weeks under well-watered conditions ($\delta^{18}O$ of tap water = -12.1 ± 0.5‰; mean $\pm$ SD), with minimum and maximum greenhouse air temperature of 17.8 ± 1.6 °C and 26.2 ± 4.8 °C, respectively, and relative humidity (RH) ranging between $52 \pm 11.9\%$ and $84.9 \pm 4.5\%$ (mean $\pm$ SD). The maximum daily photosynthetic photon flux density (PPFD) in the greenhouse averaged 975 µmol·m^{-2}·s^{-1}. All soils/hydroponics were covered with aluminium foil a day before the experiment to prevent ^{18}O label from the fog being taken up by the roots.

The 9-hr fog experiment started with a pretreatment sampling at 08:30 a.m., when leaf material from all plants was sampled. At 09:30 a.m., all plants were quickly transferred to an adjacent 14-m^2 greenhouse (i.e., fog chamber) containing ^{18}O-labelled water vapour at high humidity provided by nebulizers (Defensor 3001, Condair, Pfaeffikon, SZ, CH). The nebulizers were placed in a water bath that was constantly filled with ^{18}O-depleted water ($\delta^{18}O = -202.2$‰). Air mixing was facilitated by several fans (ø = 30 cm). To account for within species variability in $\delta^{18}O$ values of leaf water and assimilates, seven species from seven different growth forms were replicated ($n = 5$ individuals), with the individuals distributed at different locations within the fog chamber. The leaf material from the replicated plant species were sampled at five points in time (10:30 a.m., 12:30 p.m., 2:30 p.m., 4:30 p.m., and 6:30 p.m.), whereas the leaf material from all other species were sampled only at 6:30 p.m. (i.e. 9 hr after labelling start).

Sampled leaf material was immediately transferred to 12 ml gas-tight glass vials (Labco, Lampeter, UK), frozen in LN$_2$, and stored at -20°C for further analysis. The leaf material collected during the fog exposure was generally observed to be wet on the surface and was thus dried with soft paper tissues before being transferred to vials. During the 9-hr fog exposure, RH was constantly above 98% with minimum temperatures of 20.5°C at 09:30 a.m. and maximum temperatures of 33°C at 4:30 p.m. The average PPFD during the fog event was about 275 µmol·m^{-2}·s^{-1}, with a maximum PPFD of 1,122 µmol·m^{-2}·s^{-1} at 2:45 p.m.

2.2 | Isotope analysis of water vapour, leaf water, and assimilates

$\delta^{18}O$ of atmospheric water vapour was continuously monitored during the experiment using a laser spectrometer (L2120-i, Picarro, Inc., Santa Clara, CA, USA). Vapour was drawn with a flow rate of 0.25 L min^{-1} directly into the spectrometer for continuous measurement of water isotopologues. Calibration was carried out to account for the effects of changing gas concentrations, as well as to determine span and offset. The measurement precision was typically <0.3‰ (SD).

Leaf water was extracted using vacuum distillation (Lehmann et al., 2018; West, Patrickson, & Ehleringer, 2006). Analysis of $\delta^{18}O$ of water samples was performed on a thermal combustion/elemental analyser coupled to a DELTA^{PLUS}XP isotope ratio mass spectrometer (temperature conversion elemental analyser-IRMS; all Finnigan MAT, Bremen, Germany). Measurement precision was typically <0.3‰ (SD).

The dried leaf material from the glass vials was milled to a fine powder, and 60 mg of this powder was used for extraction of the water soluble compounds (WSC) in 1.5 ml deionized water at 85°C for 30 min. The neutral sugar fraction (defined here as "sugars") was isolated from the WSC using ion-exchange chromatography (OnGuard II A, H, and P; Dionex, Thermo-Fisher, Bremen, Germany) to remove ionic and phenolic compounds (Rinne, Saurer, Streit, & Siegwolf, 2012). For $\delta^{18}O$ and $\delta^{13}C$ analyses, WSC and sugars aliquots were injected into silver capsules, frozen, and freeze dried. The assimilates were pyrolyzed at 1,420°C (PYRO cube, Elementar, Hanau, Germany) and the CO gas delivered to an IRMS (Weigt et al., 2015). The measurement precision was typically <0.4‰ (SD) for oxygen and carbon isotopes. No significant oxygen isotope fractionation was observed during sugar purification (Lehmann et al., 2016; Lehmann, Gamarra, Kahmen, Siegwolf, & Saurer, 2017).

$\delta^{18}O$ values of glucose and sucrose were analysed before and after the 9-hr labelling event by gas chromatography (GC)/pyrolysis-IRMS for 38 species of eight different growth forms. An aliquot of sugars per sample (~2 mg DW^{-1}) was transferred to a 2 ml reaction vial, frozen, freeze dried, and then methylated (Lehmann et al., 2016; Lehmann et al., 2017). Methylated sugars were injected (splitless at 250° C) and separated on a 60 m, 0.25 mm, and 0.25 µm ZB-SemiVolatiles GC column (Zebron, Phenomenex, Torrance, CA, USA) in a Trace GC Ultra gas chromatograph. The sugar derivatives were pyrolyzed at 1,280°C in a commercially available oxygen isotope reactor, and the CO gas transferred via a reference unit to an IRMS (all GC/pyrolysis-IRMS parts supplied by ThermoFisher, Bremen, DE). A liquid nitrogen trap was used to ensure that no pyrolysis by-products reached the IRMS, resulting in improved precision. All samples were measured three times within a sample sequence. Interspersed sugar standard mixes of different concentrations were used for drift and amount corrections (Lehmann et al., 2016). The average measurement precision (SD) was 0.5‰ for glucose and 0.3‰ for sucrose. All $\delta^{18}O$ and $\delta^{13}C$ values are reported relative to the international Vienna Standard Mean Ocean Water or Vienna Pee Dee Belemnite scale, respectively.

2.3 | Analyses of leaf gas exchange, leaf traits, and leaf sugar pool size

Leaf gas exchange parameters, including the net assimilation rate (A_n), stomatal conductance (g_s), and transpiration rate (E), were determined a week before the labelling event over the course of several days between 10:30 a.m. and 3:30 p.m. using an infrared gas analyser with a 6 cm^2 leaf cuvette (Li-Cor 6400, Li-Cor Biosciences, Lincoln, NE, USA). It should be noted that leaf gas exchange measurements are highly challenging in wet air and that gas exchange parameters under control conditions only reflect an approximate of those under fog exposure. Fully developed leaf material was enclosed in the cuvette and when stable cuvette conditions were observed, five-point measurements per sample were taken in a 10-s interval and average values calculated for each parameter. Cuvette conditions were set to an atmospheric CO_2 concentration of 400 µmol mol^{-1}, PPFD of 1,200 µmol m^{-2} s^{-1}, and a flow rate of 500 µmol s^{-1}. Across all measurements, we maintained an RH of 54.1 ± 8.2%, a leaf temperature of 25.9 ± 1.9°C, and a leaf-to-air vapour pressure deficit of 1.7 ± 0.4 kPa. The gas exchange of some succulent and almost all epiphyte plant species could not be analysed due to low gas exchange fluxes and/or a leaf form that did not fit the leaf cuvette.

The leaf area (LA) and fresh weight (FW) of the leaf material used for gas exchange measurements were determined by a leaf area measurement device (Li-Cor 3000, Li-Cor Biosciences, Lincoln, NE, USA) and an analytical balance. Subsequently, the leaf material was dried in an oven at 60°C until stable weight to determine the dry weight (DW). Leaf succulence (L_S) was calculated according to Mantovani (1999).

$$L_S = (FW - DW)/LA. \tag{3}$$

Leaf thickness (L_{Th}) from all species was determined using a micrometer screw gauge (Mitutoyo, Kawaski, Japan). Stomatal density (S_D) and size (S_S) of the abaxial leaf side were determined from leaf impressions made using clear nail polish, mounted to slides, and subsequently observed using a light microscope (Camargo & Marenco, 2011). S_D was observed with a magnification of 20 to 40× by counting the number of stomata in a specific area (~0.175 mm^2), whereas S_S was determined in the same area by measuring the length of the stomatal aperture (n = 3 stomata per plant species). $\delta^{13}C$ analysis was used to identify different PM following O'Leary (1988). The leaf sugar pool size (i.e, [Sugars]) at the end of fog exposure was photometrically determined following the protocol of Schönbeck et al. (2018).

2.4 | Data analysis and statistics

To quantify the effects of labelling, $\delta^{18}O$ values of leaf water and assimilates during the 9-hr fog event were corrected for natural isotope abundances (Lehmann et al., 2018).

$$\Delta\delta^{18}O = \delta^{18}O_{fog} - \delta^{18}O_{prefog}, \tag{4}$$

where $\delta^{18}O_{fog}$ is the isotope ratio of a sample taken during or at the conclusion of the 9-hr labelling period and $\delta^{18}O_{prefog}$ is the isotope ratio of a sample taken before labelling start (at 08:30 a.m.).

Following Equation (4), we calculated a mean $\Delta\delta^{18}O$ value of atmospheric water vapour ($\Delta\delta^{18}O_{MV}$).

$$\Delta\delta^{18}O_{MV} = \delta^{18}O_{V-fog} - \delta^{18}O_{V-prefog}, \tag{5}$$

where $\delta^{18}O_{V-fog}$ is the average $\delta^{18}O$ value of water vapour of the last 6 hr of the experiment (−122.7‰ ± 7.2‰) when $\delta^{18}O_V$ variations were low (see Figure 1) and temperature (~31°C) and humidity were constant (RH > 98%) and where $\delta^{18}O_{V-prefog}$ is the average $\delta^{18}O$ value of water vapour of a 30-min period measured in the morning before the fog event started (−16.0 ± 0.5 ‰; both mean ± SD). The resultant $\Delta\delta^{18}O_{MV}$ value of −106.7 ± 7.2‰ reflects the isotopic labelling signal applied to the plants and denotes also the value expected for full isotopic equilibration between water vapour and leaf water. The $\Delta\delta^{18}O_{MV}$ value is thus used as a reference for this study.

The MRT of O in leaf water and assimilates during fogging were derived from exponential decay functions (Epron et al., 2012; Ruehr et al., 2009). The functions were fitted to $\Delta\delta^{18}O_{LW}$ and $\Delta\delta^{18}O_{Sugars}$ values of the species sampled over the course of the 9-hr labelling period (Figure 1).

$$\Delta\delta^{18}O\,(t) = \Delta\delta^{18}O_0 \times e^{(-\lambda \times t)} + C, \tag{6}$$

where $\Delta\delta^{18}O\,(t)$ is the quantity of ^{18}O after a given time (t), $\Delta\delta^{18}O_0$ is the initial quantity of ^{18}O at t = 0, λ is the decay rate (per hour), and C is the $\Delta\delta^{18}O_{MV}$ value to correct for negative values. MRT was calculated as $1/\lambda$ and then linearly related to $\Delta\delta^{18}O$ values at 9 hr after labelling start for each species (Figure S1). Linear regressions of these relationships were then used to model MRT_{LW} and MRTs of WSC (MRT_{WSC}) and sugars (MRT_{Sugars}) for all other species and growth forms (Table 1). With an alternative approach, on the basis of gas exchange and pool sizes, we calculate the turnover time (L_S/E) for the transpirational net flux of water going through leaf water before the fog period as the ratio of L_S (mol H_2O m^{-2}) to E (mol H_2O m^{-2} s^{-1}) following Cernusak et al. (2008). If not mentioned otherwise, one-way analysis of variance and Tukey honestly post hoc were used to test for significant differences in isotope values, MRT values, L_S/E, leaf gas exchange, leaf traits, and [Sugars] among the growth forms.

3 | RESULTS

3.1 | Temporal variations in $\Delta\delta^{18}O$ of leaf water and assimilates during fog treatment

After transferring the plants to the fog chamber at 09:30 a.m., the ^{18}O-depleted water vapour decreased for 3 hr and stabilized at 12:30 p.m. with constant values until the end of the experiment at 6:30 p.m. ($\Delta\delta^{18}O_V$; Figure 1a, grey line). The $\Delta\delta^{18}O$ values of leaf water ($\Delta\delta^{18}O_{LW}$) showed a decreasing trend during the first few hours of the experiment in six of the seven selected species that were sampled in replicate at multiple times (Figure 1a). Full equilibration

TABLE 1 Mean residence time of O in leaf water, water soluble compounds, and sugars during 9 hr of fog exposure with an ^{18}O-depleted water vapour

Growth form (species)	Leaf water		WSC		Sugars	
	$\Delta\delta^{18}O_{Max}$ (‰)	MRT_{LW} (h)	$\Delta\delta^{18}O_{Max}$ (‰)	MRT_{WSC} (h)	$\Delta\delta^{18}O_{Max}$ (‰)	MRT_{Sugars} (h)
Aquatic (*Pistia stratiotes*)	−91.5	2.9	−8.3	91.0	−16.2	37.9
Conifer (*Pinus sylvestris*)	−101.2	1.9	−9.1	90.9	−21.5	37.2
Epiphyte (*Tillandsia usneoides*)	−101.9	1.5	−11.4	72.4	−19.6	39.0
Grass (*Chasmanthium latifolium*)	−105.8	1.3	−25.3	32.0	−42.0	17.4
Shrub (*Corylus avellana*)	−104.0	1.2	−22.6	38.1	−43.2	15.3
Tree (*Fagus sylvatica*)	−105.9	1.1	−21.3	40.1	−42.3	16.3
Linear model	$y = 0.12x + 14.06$		$y = 3.58x + 119.23$		$y = 0.91x + 55.24$	
r^2	.95		.98		.98	

Note. MRT (mean residence time) values are derived from the decay constant $(1/\lambda)$ of exponential decay functions (Equation 6) that were fitted to $\Delta\delta^{18}O$ values of leaf samples of different plant species, which were taken during the labelling period (see also Figure 1). All fits were very significant ($p < .05$). The derived MRT values were related to mean $\Delta\delta^{18}O$ values at 9 hr after labelling start of the same species ($\Delta\delta^{18}O_{Max}$; Figure S1). Corresponding linear models and their regression coefficient (r^2) are given. The linear models were used to calculate MRT values in leaf water and assimilates for all other individual species and growth forms of this study.

Abbreviations: LW, leaf water; WSC, water soluble compounds.

between the $\Delta\delta^{18}O_{MV}$ reference and $\Delta\delta^{18}O_{LW}$ was observed after 3 to 7 hr, with a linear change rate of about 15.2‰ to 35.6‰ hr^{-1}.

$\Delta\delta^{18}O$ values of the water-soluble organic compounds ($\Delta\delta^{18}O_{WSC}$) generally showed a linear decrease during the 9-hr fog event. However, the ^{18}O-signal transfer to assimilates was different among the growth forms (Figure 1b). At the end of the fog exposure, $\Delta\delta^{18}O_{WSC}$ values of aquatic, conifer, and epiphyte plant species ranged between −8.3‰ and −11.4‰, whereas grass, broadleaf shrub, and broadleaf tree species ranged between −21.3‰ and −25.3‰. Similar temporal trends to $\Delta\delta^{18}O_{WSC}$ were observed in the further purified neutral sugar fraction ($\Delta\delta^{18}O_{Sugars}$), with a much stronger ^{18}O depletion and thus ^{18}O-label incorporation, allowing a clearer distinction between the growth forms (Figure 1c). The strongest ^{18}O-signal transfer to sugars was observed in grass, broadleaf shrub, and broadleaf tree species ($\Delta\delta^{18}O_{Sugars}$ of approximately −42.5‰, with a linear change rate of 4.7‰ hr^{-1}), and the ^{18}O-label incorporation was approximately two times lower in aquatic, conifer, and epiphyte species ($\Delta\delta^{18}O_{Sugars}$ of approximately −19.1‰, with 2.1‰ hr^{-1}). In agreement with the effect of $\delta^{18}O_V$ on leaf water, the succulent species showed no clear ^{18}O-signal transfer to WSC and sugars. The average standard errors for $\Delta\delta^{18}O_{LW}$, $\Delta\delta^{18}O_{WSC}$, and $\Delta\delta^{18}O_{Sugars}$ for each point in time, across all seven replicated plant species, were 3.2‰, 1.3‰, and 2.8‰, respectively. These indicate that the position within the fog chamber, the diurnal variability in light conditions, and the within-species variability resulted in low uncertainty for ^{18}O-signal transfer processes.

3.2 | ^{18}O-signal transfer to leaf water and assimilates across 140 species

We sampled leaf material before and at the end of fog exposure and measured $\Delta\delta^{18}O$ values of leaf water and assimilates in 140 plant species. $\Delta\delta^{18}O_{LW}$ values showed a nonlinear relationship with $\Delta\delta^{18}O_{Sugars}$ across all species (Figure 2a). Plants with the highest ^{18}O-label uptake to leaf water (i.e., close to the $\Delta\delta^{18}O_{MV}$ reference of −106.7‰ ± 7.2; mean ± SD) showed a higher variability in $\Delta\delta^{18}O_{Sugars}$. We expected full isotopic equilibrium between water vapour and leaf water after a 9-hr fog period at high humidity conditions ($e_a/e_i = 1$) and thus $\Delta\delta^{18}O_{LW}$ values to be similar to the $\Delta\delta^{18}O_{MV}$ reference (Lehmann et al., 2018). Surprisingly, $\Delta\delta^{18}O_{LW}$ values in only 54% of all measured species (i.e., 74 out of 137) were similar to the $\Delta\delta^{18}O_{MV}$ reference (within 1 SD). In contrast, $\Delta\delta^{18}O_{LW}$ values in 22% and in 24% of all measured species (i.e., 30–33 out of 137) were only near (within 2 to 3 SD) or far off (outside 3 SD) the $\Delta\delta^{18}O_{MV}$ reference, respectively, and thus not in full equilibrium with $\Delta\delta^{18}O_V$. Mean $\Delta\delta^{18}O_{LW}$ values of most growth forms ranged between −93.0‰ and −103.5‰ and were similar or only slightly off (e.g., aquatics and herbs) the $\Delta\delta^{18}O_{MV}$ reference (Figure 2b; Table 2). Mean $\Delta\delta^{18}O_{LW}$ values of −27‰ and −52.7‰ in succulents and epiphytes differed clearly from the $\Delta\delta^{18}O_{MV}$ reference and were thus not in full isotopic equilibrium with water vapour. In addition, oxygen and hydrogen isotopes in leaf water showed a clear 1:1 relationship after a 9-hr fog exposure (Figure S2).

The mean $\Delta\delta^{18}O$ values of WSC and sugars were highly variable among growth forms and ranged from −3.0‰ to −42.2‰ (Figure 2b; Table 2), with the strongest ^{18}O-signal transfer in grasses and aquatics and the lowest in epiphytes and succulents. Although compound-specific analysis revealed no clear growth form differences for mean $\Delta\delta^{18}O$ values of glucose and sucrose (Figure 2b; Table 2), sucrose was generally the compound that was most ^{18}O-labelled at the end of fog exposure. Sucrose was on average 6.6‰, 11.9‰, and 17.3‰ more negative at the end of fog exposure than total sugars, glucose, and WSC across all growth forms, respectively. For prelabelling conditions (i.e., natural abundance), sucrose was on average 6.7‰, 8.5‰, and 40.1‰ enriched in ^{18}O compared with glucose, sugars, and leaf water across all growth forms (data not shown). Thus, sucrose was
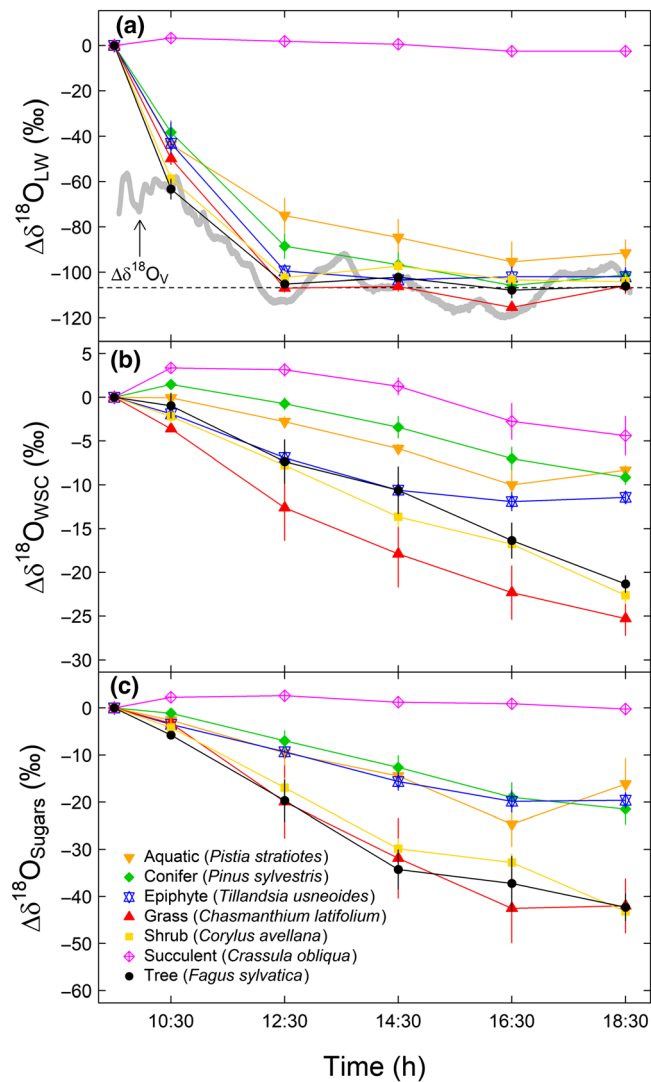
FIGURE 1 Temporal $\Delta\delta^{18}O$ variations during 9 hr of fog exposure with ^{18}O-depleted water vapour. $\Delta\delta^{18}O$ values of (a) leaf water, (b) water soluble compounds, and (c) sugars of different growth forms before and during the fog event are shown. The ^{18}O-depleted fog source water ($\Delta\delta^{18}O_V$) is indicated by the solid grey line in the upper panel. The mean $\Delta\delta^{18}O$ value of water vapour ($\Delta\delta^{18}O_{MV} = -106.7‰$) is indicated by the dashed black line, reflecting a reference for full isotopic equilibration between leaf water and water vapour. Means ± 1 standard error are given ($n = 3$–5 replicates per species)

the most ^{18}O-enriched compound for prelabelling conditions and showed the highest ^{18}O-label incorporation after fog exposure across all compounds.

3.3 | MRT values in relation to potential leaf traits and physiological drivers

MRT_{LW} values derived from $\Delta\delta^{18}O_{LW}$ values at the end of fog exposure and L_S/E values derived from L_S and E data before the fog ranged between 1.4 and 10.8 hr (Figure 3a). MRT_{LW} varied among growth forms ($p < .001$) but not L_S/E ($p > .05$). No clear relationship between

both MRT_{LW} and L_S/E were observed ($r^2 < .11$ and $p < .001$). Moreover, MRT_{WSC} and MRT_{Sugars} differed clearly among growth forms ($p < .001$), with the highest values in epiphytes and succulents and lowest in grasses and aquatics, ranging between 32.5 and 108.5 hr for MRT_{WSC} and 15.5 and 51.9 hr for MRT_{Sugars} (Figure 3b).

Leaf traits and physiological drivers potentially influencing the ^{18}O-signal transfer and thus the MRT in leaf water and assimilates varied among plant species and growth forms (Table 3). We found significant variation in leaf stomatal conductance (g_s), transpiration (E), stomatal density (S_D), stomatal size (S_S), leaf succulence (L_S), and leaf thickness (L_{Th}) but not in photosynthesis (A_n) and leaf sugar pool size ([Sugars]), as a function of different growth forms (Table 3). Stomatal density (S_D) and size (S_S) were negatively correlated ($R = -.55$), whereas metrics of leaf water content, such as L_S and leaf thickness (L_{Th}) were positively correlated ($R = .61$; Figure S3). The collinearity between similar traits indicates the difficulty in ultimately disentangling which anatomical or morphological traits are most closely related to variation in residence time.

MRT_{LW} values were weakly influenced by anatomical leaf traits such as stomatal density (S_D) and size (S_S) (Figures 4a,b; $r^2 \leq .11$), but strongly by morphological leaf traits such as L_S and L_{Th} (Figures 4c,d; $r^2 \leq .46$). However, MRT_{LW} values varied significantly as a function of the interaction between growth form and a given leaf trait ($p < .02$ for S_D, L_S, or L_{Th}), with the interaction effects beeing largely driven by the succulent growth form. The anatomical and morphological leaf traits were also related to MRT_{WSC} and MRT_{Sugars} but weaker than with MRT_{LW} (Figure S3). Moreover, neither leaf gas exchange parameters (measured under controlled conditions) nor [Sugars] showed a clear relationship with MRT in assimilates (Figure S3). In addition, we used the relationship between MRT_{Sugars} and $\delta^{13}C$ of sugars to identify PM for each species. (Figure S4; Table S1). We found that PM influenced the MRT in leaf water and assimilates (Table 4). C_4 plants showed the lowest MRT_{WSC} and MRT_{Sugars} values, and MRT_{LW} values were similar between C_3 and C_4 plants. In contrast, succulent and epiphyte CAM plants showed the highest MRT_{LW}, MRT_{WSC}, and MRT_{Sugars} values; however, it should be considered that the experimental fogging occurred during daytime and not during nighttime, when CAM plants actively open their stomata for CO_2 assimilation. Besides, MRT_{Sugars} values were clearly lower compared with MRT_{WSC} values across all PMs.

4 | DISCUSSION

4.1 | Leaf water content influences the MRT of O in leaf water

Figure 1a shows that full isotopic equilibrium between water vapour and leaf water (i.e., $\Delta\delta^{18}O_{MV}$) was generally reached within 3–7 hr in the fog. This is consistent with previous observations showing that it takes several hours for leaf water pools to achieve full isotopic equilibrium and thus steady-state conditions after a step change in $\Delta\delta^{18}O_V$ (Kim & Lee, 2011; Lehmann et al., 2018; Roden & Ehleringer, 1999).
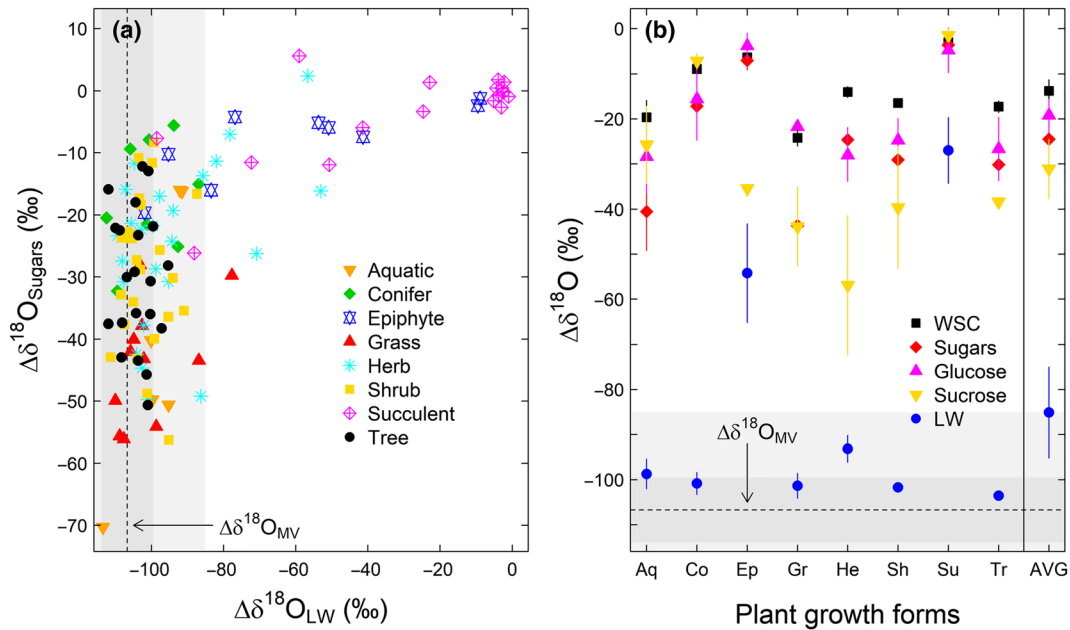
FIGURE 2 $\Delta\delta^{18}O$ values of leaf water and assimilates at the end of 9-hr fog exposure with ^{18}O-depleted water vapour. (a) Relationships between $\Delta\delta^{18}O$ values of leaf water ($\Delta\delta^{18}O_{LW}$) and $\Delta\delta^{18}O$ values of sugars ($\Delta\delta^{18}O_{Sugars}$) across individual plant species of eight different growth forms. (b) Mean $\Delta\delta^{18}O$ values ± 1 standard error of leaf water (LW), water soluble compounds (WSC), sugars, glucose, and sucrose for different growth forms are given. The mean $\Delta\delta^{18}O$ value of water vapour ($\Delta\delta^{18}O_{MV}$ = −106.7‰) is indicated by the dashed black line, reflecting a reference for full isotopic equilibrium between leaf water and water vapour. The uncertainties of $\Delta\delta^{18}O_{MV}$ are denoted by dark–grey (±1 SD, 7.2‰) and light–grey (±3 SD, 21.6‰) shaded areas. Please refer to Table 2 for significant differences among growth forms and number of species per growth form. Aq = Aquatics, Co = Conifers, Ep = Epiphytes, Gr = Grasses, He = Herbs, Sh = Shrubs, Su = Succulents, Tr = Trees, and AVG = average $\Delta\delta^{18}O$ value across all growth forms [Colour figure can be viewed at wileyonlinelibrary.com]

TABLE 2 Isotope analysis of leaf water and assimilates across plant growth forms after 9-hr fog exposure with ^{18}O-depleted water vapour

Parameter F_{df} values	$\Delta\delta^{18}O_{LW}$ (‰) $F_{7,129}$ = 46.1***	$\Delta\delta^{18}O_{WSC}$ (‰) $F_{7,131}$ = 23.1***	$\Delta\delta^{18}O_{Sugars}$ (‰) $F_{7,115}$ = 19.2***	n	$\Delta\delta^{18}O_{Glucose}$ (‰) $F_{7,25}$ = 2.8*	$\Delta\delta^{18}O_{Sucrose}$ (‰) $F_{7,10}$ = 1.5$^{n.s.}$	n
Aquatic	−98.7 ± 3.3 a	−19.7 ± 3.8 ab	−40.5 ± 8.7 ab	5–6	−28.4 ± 8.2 a	−25.7 ± 8.6 a	2
Conifer	−100.8 ± 2.5 a	−8.9 ± 1.0 cd	−17.1 ± 3.3 cd	8–10	−15.6 ± 9.2 a	−7.2 ± 1.8 a	2–4
Epiphyte	−54.2 ± 10.9 b	−6.4 ± 1.4 d	−7.1 ± 2.1 d	9–11	−3.8 ± 2.9 a	−35.4 a	1–5
Grass	−101.3 ± 2.8 a	−24.2 ± 1.8 a	−43.6 ± 2.9 a	9–12	−21.7 a	−43.9 ± 8.8 a	1–2
Herb	−93.1 ± 3.0 a	−14.0 ± 1.2 bc	−24.6 ± 2.7 bc	23–28	−28.1 ± 5.8 a	−56.9 ± 15.5 a	3–5
Shrub	−101.7 ± 1.1 a	−16.5 ± 0.9 b	−29.1 ± 2.3 bc	26–29	−24.8 ± 4.9 a	−39.6 ± 13.5 a	5–6
Succulent	−27.0 ± 7.3 c	−3.0 ± 0.8 d	−3.6 ± 1.8 d	17–19	−4.8 ± 4.9 a	−1.5 ± 1.4 a	2–5
Tree	−103.6 ± 1.0 a	−17.3 ± 1.3 b	−30.2 ± 2.4 bc	21–24	−26.7 ± 7.1 a	−38.3 a	1–5
Mean ± SE	−85.1 ± 10.1	−13.8 ± 2.5	−24.5 ± 5.1	118–139	−19.2 ± 3.6	−31.1 ± 6.6	17–34

Note. $\Delta^{18}O$ values of leaf water ($\Delta\delta^{18}O_{LW}$), water soluble compounds ($\Delta\delta^{18}O_{WSC}$), and sugars ($\Delta\delta^{18}O_{Sugars}$) are shown, as well as $\Delta^{18}O$ values of the individual sugars, glucose ($\Delta\delta^{18}O_{Glucose}$) and sucrose ($\Delta\delta^{18}O_{Sucrose}$). F values, degree of freedom, and significance of one-way analysis of variance (n.s. = not significant) are given. Letters indicate significant differences among growth forms derived from Tukey-honestly significant difference post-hoc test. n denotes number of measured plant species per growth form. Means and standard error (SE) are shown.

Abbreviations: df, degree of freedom.

*p < .05. ***p < .001.

However, only 54% of all measured plant species actually reached the $\Delta\delta^{18}O_{MV}$ reference after 9 hr of fog exposure with ^{18}O-depleted water vapour source (Figure 2a; Table 2), and, in particular, many herbs, epiphytes, and succulents did not achieve full isotopic equilibrium and thus steady-state conditions. The high $\Delta\delta^{18}O_{LW}$ variability among species is also reflected in MRT_{LW} values, which ranged

between 1.4 and 10.8 hr among all tested growth forms (Figure 3a). About 50% of the MRT_{LW} variation among plant species and growth forms was explained by metrics of leaf water content such as leaf succulence (L_S) and leaf thickness (L_{Th}; Figures 4c,d). This fits well with evidence that leaf water content affects the isotopic leaf water enrichment (Cernusak et al., 2008; Ellsworth, Ellsworth, Anderson, &
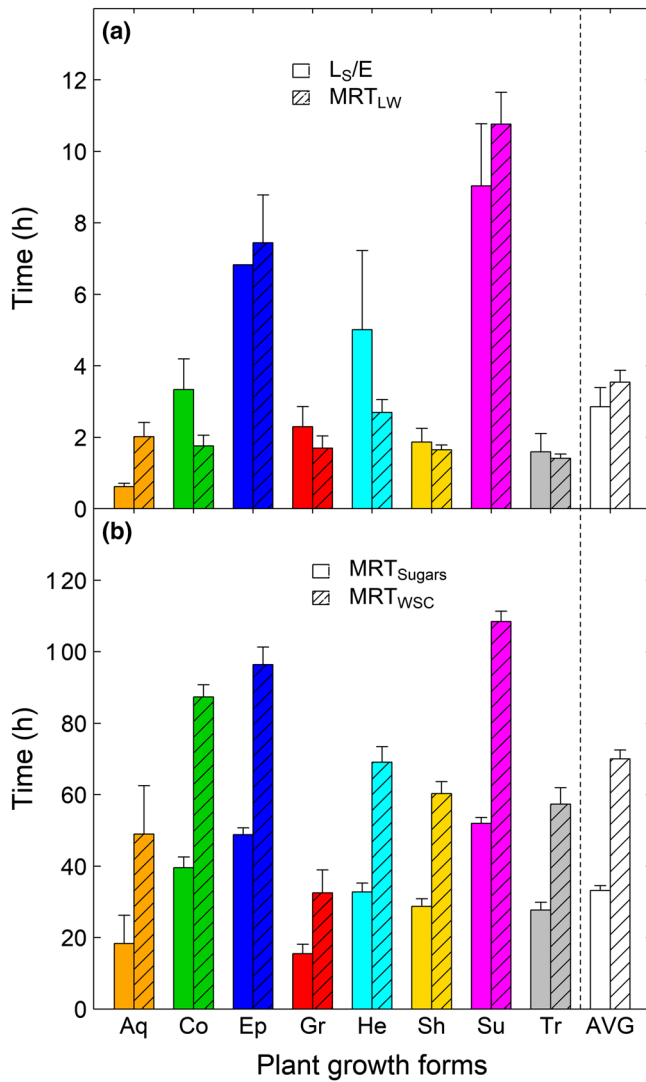
FIGURE 3 Quantification of ^{18}O-signal transfer from vapour to leaf water and assimilates across different plant growth forms. (a) Mean residence time of O in leaf water (MRT_{LW}) during a fog event and turnover time of leaf water (L_S/E) before the fog event. (b) Mean residence time of O in sugars (MRT_{Sugars}) and water soluble compounds (MRT_{WSC}). Please refer to Table 2 for significant differences among growth forms and number of species per growth form. It should be considered that the experimental fogging period occurred during daytime and not during nighttime, when the majority of species in the succulent and epiphyte growth form actively open their stomata for CO_2 assimilation due to the photosynthetic crassulacean acid metabolism mechanism. Aq = Aquatics, Co = Conifers, Ep = Epiphytes, Gr = Grasses, He = Herbs, Sh = Shrubs, Su = Succulents, Tr = Trees, and AVG = average across all growth forms [Colour figure can be viewed at wileyonlinelibrary.com]

Sternberg, 2013; Liang et al., 2018) and the $\delta^{18}O$ of transpired water (Dubbert et al., 2017; Simonin et al., 2013; Song, Simonin, Loucos, & Barbour, 2015). High leaf water content likely causes a stronger dilution of the ^{18}O label, explaining the increase in MRT_{LW} with L_S. Given the influence of leaf water content on MRT_{LW} and thus on steady-state conditions between water vapour and leaf water, nonlinear steady-state models (Song et al., 2015) should probably be used in

TABLE 3 Leaf gas exchange parameters, leaf traits, and leaf sugar pool size across different plant growth forms

Parameter F_{df} values	A_n (μmol m^{-2} s^{-1}) $F_{7,101} = 1.5$ n.s.	g_s (mmol m^{-2} s^{-1}) $F_{7,101} = 3.5$**	E (mmol m^{-2} s^{-1}) $F_{7,101} = 3.7$**	[Sugars] % DW $F_{7,68} = 1.1$ n.s.	S_S (μm) $F_{7,97} = 2.1$*	S_D (mm^{-2}) $F_{7,97} = 2.8$*	L_S (kg m^{-2}) $F_{7,101} = 11.7$***	L_{Th} (mm) $F_{7,131} = 13.1$***	n
Aquatic	11.0 ± 3.3 a	386.3 ± 107.7 a	5.1 ± 1.0 a	2.6 ± 0.8 a	29 ± 6.1 ab	181.9 ± 100.9 ab	0.22 ± 0.04 b	0.8 ± 0.2 b	3–6
Conifer	8.7 ± 1.0 a	105.2 ± 17.4 b	2.1 ± 0.4 b	5.3 ± 1.3 a	32.2 ± 3.2 ab	109.9 ± 15.2 ab	0.3 ± 0.05 b	0.6 ± 0.1 b	7–10
Epiphyte	3.2 a	30.0 b	0.5 b	3.3 ± 0.5 a	34 ab	91.4 ab	0.23 b	1.7 ± 0.3 b	1–11
Grass	6.7 ± 1.2 a	67.5 ± 12.1 b	1.3 ± 0.2 b	4.5 ± 1.1 a	28.5 ± 2.1 ab	170 ± 17 ab	0.13 ± 0.01 b	0.5 ± 0.1 b	10–12
Herb	5.7 ± 0.7 a	134.6 ± 28.9 b	2.0 ± 0.3 b	2.7 ± 1 a	35.9 ± 2.9 a	111.1 ± 20.2 ab	0.25 ± 0.04 b	0.8 ± 0.1 b	12–27
Shrub	7.3 ± 1.0 a	148.7 ± 34.3 b	2.2 ± 0.4 b	3.4 ± 0.7 a	31.1 ± 2.2 ab	173.1 ± 26.7 ab	0.12 ± 0.01 b	0.7 ± 0.1 b	12–30
Succulent	4.0 ± 0.1 a	43.3 ± 6.7 b	0.8 ± 0.2 b	2.3 ± 1 a	35.9 ± 2.9 a	69.3 ± 17.4 a	0.77 ± 0.21 a	3.3 ± 0.6 a	3–19
Tree	7.3 ± 0.6 a	118.7 ± 17.9 b	2.0 ± 0.2 b	3 ± 0.3 a	25.1 ± 1.6 ab	188.7 ± 23.3 a	0.11 ± 0.03 b	0.9 ± 0.1 b	13–24

Note. Net assimilation rate (A_n), stomatal conductance (g_s), transpiration rate (E), leaf sugar pool size ([Sugars]), abaxial stomatal size (S_S) and density (S_D), leaf succulence (L_S), leaf thickness (L_{Th}) are shown. F values, degree of freedom, and significance of one-way analysis of variance (n.s. = not significant) are given. Letters indicate significant differences among growth forms derived from Tukey honestly significant difference post-hoc test. n denotes number of measured species per growth form. Means ± 1 standard error are shown.

Abbreviation: DW, dry weight.

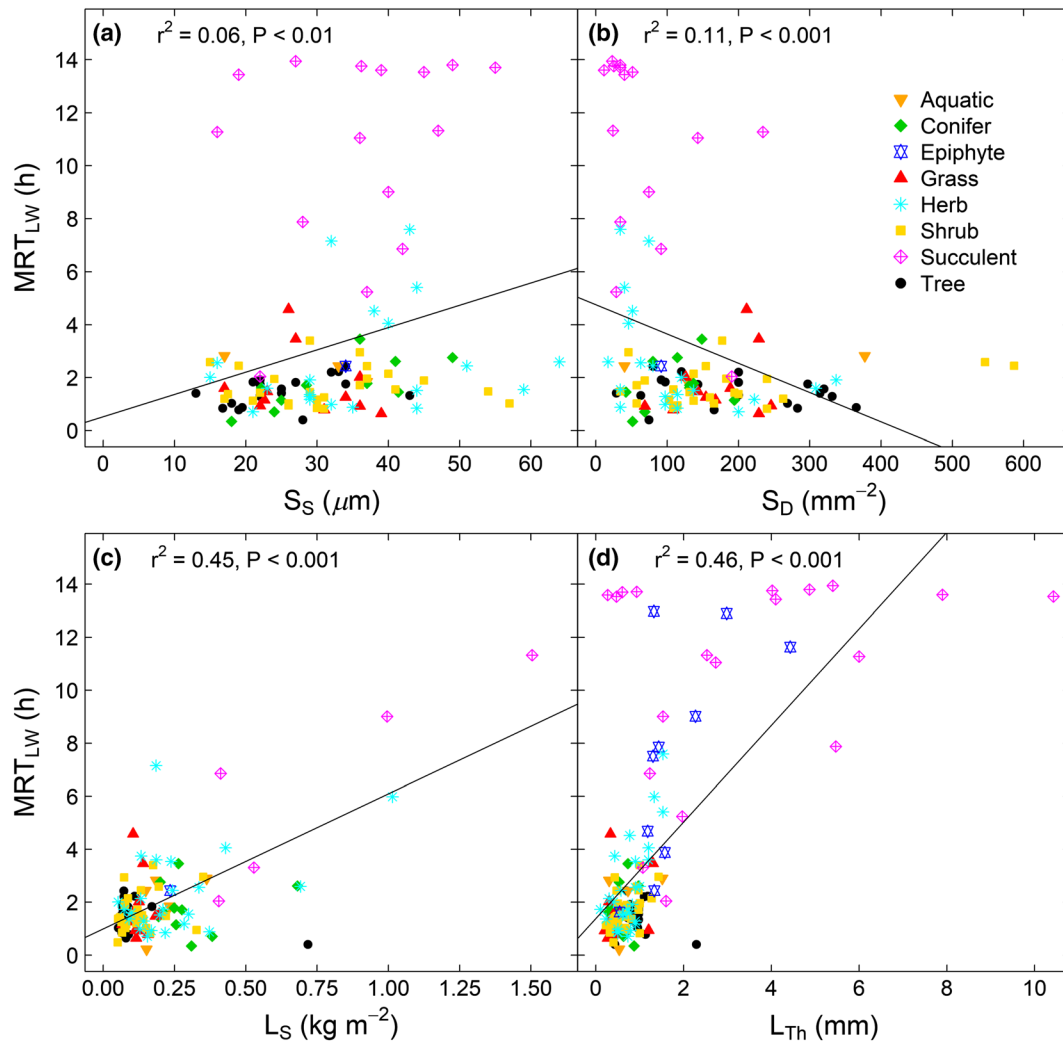*$p < .05$. **$p < .01$. ***$p < .001$.

FIGURE 4 Influence of anatomical and morphological leaf traits on mean residence time of O in leaf water (MRT_{LW}). Relationships between MRT_{LW} values and (a, b) abaxial stomatal size (S_S) and density (S_D), and (c, d) leaf succulence (L_S) and thickness (L_{Th}) across individual plant species of eight different growth forms are shown. It should be considered that the experimental fogging period occurred during daytime and not during nighttime, when the majority of species in the succulent and epiphyte growth form actively open their stomata for CO_2 assimilation due to the photosynthetic crassulacean acid metabolism mechanism [Colour figure can be viewed at wileyonlinelibrary.com]

TABLE 4 Differences in carbon and oxygen isotopic composition and mean residence times of O in leaf water and assimilates across photo-synthetic modes (PM)

PM	$\delta^{13}C_{Sugars}$ (‰)	$\delta^{18}O_{Sugars}$ (‰)	MRT_{LW} (h)	MRT_{WSC} (h)	MRT_{Sugars} (h)	n
CAM	−15.8 ± 0.5	32.9 ± 0.7	10.7 ± 0.9	102.9 ± 3.7	51.8 ± 1.2	20–21
C_4	−13.6 ± 0.8	35.6 ± 2.4	1.3 ± 0.7	12.9 ± 11.7	3.9 ± 5.0	4
C_3	−28.6 ± 0.2	29.9 ± 0.2	2.0 ± 0.1	65.4 ± 2.4	30.5 ± 1.3	93–103

Note. $\delta^{13}C$ and $\delta^{18}O$ values of sugars ($\delta^{13}C_{Sugars}$, $\delta^{18}O_{Sugars}$) were taken at 08:30 a.m. before the fog event. Mean residence time of O in leaf water (MRT_{LW}), water soluble compounds (MRT_{WSC}), and sugars (MRT_{Sugars}) are given. *n* denotes number of measured plant species per photosynthetic modes. For MRT values of crassulacean acid metabolism plants, which are derived from epiphyte and succulent growth forms, it should be considered that the experimental fogging period occurred during daytime and not during nighttime, when crassulacean acid metabolism (CAM) plants actively open their stomata for CO_2 assimilation. Means ± 1 standard error are shown.

studies including succulent species (Cernusak et al., 2008; Liang et al., 2018). In comparison, traits such as stomatal density and size were only weakly related to changes in MRT_{LW} (Figures 4a,b), implying that stomatal variations in our study are not the cause of the water vapour-

induced $\Delta\delta^{18}O_{LW}$ variations. Importantly, the influence of $\Delta\delta^{18}O_V$ on $\Delta\delta^{18}O_{LW}$ in this study should not be interpreted as net leaf/foliar water uptake (i.e., a net influx of water entering the leaf). Although we cannot fully exclude that some species actively took up water from

vapour or condensed water on leaf surfaces (Goldsmith, 2013; Gotsch et al., 2014), a passive foliar water uptake along a potential leaf water gradient is unlikely given that plants were well watered. We conclude that the isotopic equilibration between water vapour and leaf water can be influenced by the leaf water content across a wide range of plant species and growth forms. Leaf water content should therefore be taken into account in leaf water isotope models, particularly given species with different degrees of succulence.

Moreover, from an isotopic point of view, Farquhar and Cernusak (2005) calculated that the amount of water entering the leaf through the stomata can be about twice as high as the amount of xylem water entering the leaf. Neglecting differences in the response to changes in humidity conditions, the estimation of MRT_{LW} (during fog conditions) and L_S/E (before fog conditions) allow this hypothesis to be tested. Both parameters describe similar pool and flux relationships; however, we assume that both differ in their properties. MRT_{LW} values are driven by a bidirectional flux of water in the vapour phase that mixes and equilibrates with water in the liquid phase, particularly under high humidity conditions when transpiration rates are at or close to 0 (Goldsmith et al., 2017; Kim & Lee, 2011). In contrast, L_S/E values are determined by a transpirational net flux out of the leaves to the atmosphere that varies widely with leaf evaporative conditions and that depends on stomata regulation and leaf water content. L_S/E values of broadleaf trees, coniferous trees, and succulents were similar to previous studies (Cernusak et al., 2008; Dubbert et al., 2017; Dubbert, Cuntz, Piayda, & Werner, 2014) and, across all growth forms, in a similar range as MRT_{LW} (Figure 3a). As humidity increases, L_S/E values are expected to be higher (i.e., less xylem water entering the leaf), but the response of MRT_{LW} to changes in humidity is unknown. We hypothesize lower MRT_{LW} values with an increase in humidity (i.e., more vapour-derived water entering the leaf; Equation 1). The estimation by Farquhar and Cernusak (2005) might therefore be relevant under low leaf evaporative conditions, when L_S/E values are high and MRT_{LW} values are low. However, the rate of water entering the leaf from the atmosphere might not always be twice as high as the rate of water entering from roots. To better understand this, measurements of MRT_{LW} and L_S/E along a humidity gradient could be made.

4.2 | ^{18}O-signal transfer to leaf assimilates varies among plant species and growth forms

The transfer of the ^{18}O-signal from water vapour to plant assimilates differed strongly among species and growth forms (Figures 1 and 2; Table 2). This variation was also evident in MRT_{WSC} and MRT_{Sugars} (Figure 3b), demonstrating a shorter O residence time in purified sugars than in the WSC. Although the ^{18}O-label incorporation into assimilates was found to depend on RH and on the photosynthetic activity of a plant (Lehmann et al., 2018; Studer et al., 2015), studies determining the MRT of assimilates after a ^{18}O-labelling event are lacking. We therefore compared our results with those of $^{13}CO_2$ experiments (Epron et al., 2012). MRT_{WSC} values derived from decay constant values after a $^{13}CO_2$ pulse-labelling ranged between 5 to 25 hr for beech and pine saplings across the season (Desalme et al., 2017) and 57.6 hr for nondrought stressed beech saplings (Ruehr et al., 2009) and were thus lower or similar to those of the present study. MRT_{Sugars} values of broadleaf and conifer saplings ranged between 14 and 22 hr (Blessing, Werner, Siegwolf, & Buchmann, 2015; Galiano Pérez et al., 2017) and were lower compared with MRT_{Sugars} values of 28 and 40 hr for broadleaf and conifer plants in the present study, respectively. However, MRT values of assimilates likely depend on the experimental conditions, and the incorporation rate and allocation processes might differ between ^{13}C and ^{18}O labels, as observed in a multi-isotope labelling experiment (Studer et al., 2015).

MRT values of leaf water and assimilates revealed the fast-growing aquatics and grasses to be the most sensitive growth forms to $\delta^{18}O_V$ variations (Figure 3). Species of these growth forms might therefore be useful candidates for tracing and reconstructing hydrological signals from water vapour sources in humid environments (Hu & Riveros-Iregui, 2016). However, it should also be noted that individual broadleaf tree, shrub, and herb species showed a relatively strong ^{18}O-signal transfer that was similar to grasses and aquatics (Figure 2 a). Thus, other plant species can also be used to determine and trace water vapour isotopic signals from plant organic matter (Helliker & Griffiths, 2007).

Moreover, the observed differences in the ^{18}O-signal transfer to sugars among plant species and growth forms may also be attributed to the photosynthetic response of each species to the high humidity conditions (Aparecido et al., 2017; Berry & Smith, 2014; Dawson & Goldsmith, 2018; Eller et al., 2013); however, A_n was not related to $\Delta\delta^{18}O_{Sugars}$ (and thus to MRT_{Sugars}; Figure S3). We assume that the A_n values measured before the experiment may not reflect the actual A_n values occurring during the fog event. However, given that gas exchange measurements could neither be made for all species nor during fog conditions and that control plants experiencing no fog exposure were absent, we cannot fully separate the physiological effects leading to changes in the ^{18}O-signal transfer from water vapour to assimilates. Further, we expected that the leaf sugar pool size is partially related to the ^{18}O incorporation into assimilates; however, neither [Sugars] nor the turnover time of leaf sugars (i.e., [Sugars]/A_n) showed a relationship with $\Delta\delta^{18}O_{Sugars}$ (Figure S3). The absence of a relationship might be explained by high concentrations of sugar alcohols, which are not captured by the sugar pool measurements and have a much longer O residence time compared with sucrose and glucose (Lehmann et al., 2018) or by species-specific differences in the relative concentration of compounds and in allocation of recent assimilates towards respiration or carbon sinks (Epron et al., 2012).

However, the nonlinear relationship between $\Delta\delta^{18}O_{LW}$ and $\Delta\delta^{18}O_{Sugars}$ and by extension between MRT_{LW} and MRT_{Sugars} across all species and growth forms can be partially explained by mechanistic differences in CO_2 uptake during photosynthesis (Figure 2a). It should be considered that high MRT values in leaf water and sugars for epiphyte and succulent growth forms are caused by their photosynthetic CAM mechanism (Figures 3 and 4; Table 4), which has been confirmed for the majority of species in both growth forms (Figure S4; Table S1).

CAM plants open their stomata for CO_2 assimilation mainly at night-time; however, the experimental fogging was conducted during daytime. Nevertheless, some epiphyte or succulent CAM plants may have opened their stomata during daytime fogging (Phase II or IV of the CAM mechanism) and therefore have incorporated some [18]O label into water and sugars (Figure 2a; Table 2). Interestingly, the CAM epiphyte *Tillandsia usneoides*, which has been described as plant species that integrates the water vapour signal over time (Helliker, 2014), was found to be an exception (Figure 1a). We assume that this was caused by a lower leaf water content, causing a higher ^{18}O-label uptake via water vapour compared with other CAM plants. Uptake of condensed water through the base of water-absorbent epidermal trichomes might also explain the strong ^{18}O-signal transfer in *T. usneoides*, independent of stomatal opening. In contrast, C_4 plant species are often characterized by higher assimilation rates and faster growth in comparison with C_3 plants, explaining why these plants show the shortest MRT_{WSC} and MRT_{Sugars} and thus the fastest ^{18}O-signal transfer to assimilates among all PM. Whether or not C_3 and C_4 plant species of the same growth form differ in their ^{18}O-label uptake requires further research.

4.3 | $\delta^{18}O$ of sucrose as a sensitive tool to determine $\delta^{18}O$ variations in leaf water

Interestingly, across all growth forms, sucrose was on average the most ^{18}O-labelled compound after the fog exposure (Figure 2b; Table 2) but also the most ^{18}O-enriched compound at natural isotope abundances. This confirms previous studies measuring $\delta^{18}O$ values in individual carbohydrates of grass and tree species (Lehmann et al., 2017; Lehmann et al., 2018) and shows that the findings can be extended to a wider range of species and growth forms. It also demonstrates that sucrose is more sensitive to isotopic variations in water vapour and leaf water compared with other assimilates. We assume that the higher ^{18}O-label incorporation and [18]O enrichment in sucrose compared with other carbohydrates and metabolic fractions might be connected via processes occurring close to the site of evaporation in the stomatal cavity, where the transpirational water loss and the exchange between water vapour and leaf water occur. The synthesis of sucrose might be closely linked to the production of triose phosphates that have been photosynthetically produced in strongly ^{18}O-enriched water or, in extension, in ^{18}O-labelled leaf water. Glucose might be disconnected from recent photosynthetic fluxes and functioning in either osmolytic processes (Lehmann et al., 2015; Rinne et al., 2015) or as a carbon storage pool with a slower turnover time that is mainly laid down in the vacuole (Nadwodnik & Lohaus, 2008). In addition, hexoses such as glucose may lose their original leaf water signal faster than sucrose due to isotope exchange processes (Sternberg, DeNiro, & Savidge, 1986). Oxygen isotopes in aldehyde and ketone groups of hexoses can be exchanged with those in surrounding water (Schmidt, Werner, & Rossmann, 2001; Werner, 2003), explaining oxygen isotope fractionations among individual leaf sugars (Lehmann et al., 2017). It also explains why the isotopic leaf

water signal in assimilates is partially obscured by unenriched xylem water before incorporation into structural plant components such as leaf or tree-ring cellulose (Barbour & Farquhar, 2000; Roden et al., 2000). Thus, our results suggest $\delta^{18}O$ analysis of sucrose as the most sensitive compound that can be traced throughout the plant for reconstruction of climatic and hydrological conditions (Gessler et al., 2013; Treydte et al., 2014).

5 | CONCLUSIONS AND IMPLICATIONS

Our multispecies approach showed that the ^{18}O-signal transfer from water vapour via leaf water to sugars under high humidity conditions varies substantially among plant species and growth forms. Our results need to be considered in experiments focusing on water dynamics in plants varying in leaf succulence and thickness or where differences in PM are expected (i.e., comparison of $\delta^{18}O$ values in leaf water among growth forms, e.g., host vs. parasitic plants and mature trees vs. herbs/grasses of the understorey). Moreover, because the $\delta^{18}O$ values of plant assimilates ultimately shape $\delta^{18}O$ values of plant compounds (Gessler et al., 2014; Hepp et al., 2015; Zech et al., 2013), measuring the $\delta^{18}O$ of sucrose and its incorporation into tree-ring cellulose along vertical gradients within individual trees might be a good starting point to trace the isotopic signal of water vapour and its environmental–hydrological information (e.g., weather and climatic conditions and atmospheric circulations patterns). Given the close relationship between oxygen and hydrogen isotopes after fog exposure (Figure S1), water vapour-induced changes in δ^2H values of leaf water might be also imprinted on δ^2H biomarker such as fatty acids or *n*-alkanes (Cormier et al., 2018; Gamarra, Sachse, & Kahmen, 2016; Sachse et al., 2012), providing a new avenue for the reconstruction of hydrological information. Future studies should therefore include water vapour isotope measurements, particularly, in naturally humid environments such as coastal regions, cloud forests, or during intense periods of precipitation to better understand the transfer of isotopic signals under field conditions. Finally, it should be noted that the [18]O labelling via water vapour is an easy-to-apply method, which gives versatile information on water and carbon dynamics in plants and can also be combined with $^{13}CO_2$ or $^{14}CO_2$ labelling to simultaneously trace the C, O, and H of fresh assimilates among different tissues.

AUTHOR CONTRIBUTIONS

ORCID

Marco M. Lehmann https://orcid.org/0000-0003-2962-3351
Gregory R. Goldsmith https://orcid.org/0000-0003-3567-8949
Leonie Schönbeck https://orcid.org/0000-0001-9576-254X
Matthias Saurer https://orcid.org/0000-0002-3954-3534

REFERENCES

Aparecido, L. M. T., Miller, G. R., Cahill, A. T., & Moore, G. W. (2017). Leaf surface traits and water storage retention affect photosynthetic responses to leaf surface wetness among wet tropical forest and semi-arid savanna plants. *Tree Physiology, 37*, 1285–1300. https://doi.org/10.1093/treephys/tpx092

Barbour, M. M., & Farquhar, G. D. (2000). Relative humidity- and ABA-induced variation in carbon and oxygen isotope ratios of cotton leaves. *Plant, Cell & Environment, 23*, 473–485. https://doi.org/10.1046/j.1365-3040.2000.00575.x

Berry, Z. C., Emery, N. C., Gotsch, S. G., & Goldsmith, G. R. (2018). Foliar water uptake: Processes, pathways, and integration into plant water budgets. *Plant, Cell & Environment, 42*(2), 410–423.

Berry, Z. C., & Smith, W. K. (2014). Experimental cloud immersion and foliar water uptake in saplings of *Abies fraseri* and *Picea rubens*. *Trees-Structure and Function, 28*, 115–123. https://doi.org/10.1007/s00468-013-0934-5

Blees, J., Saurer, M., Siegwolf, R. T. W., Ulevicius, V., Prevôt, A. S. H., Dommen, J., & Lehmann, M. M. (2017). Oxygen isotope analysis of levoglucosan, a tracer of wood burning, in experimental and ambient aerosol samples. *Rapid Communications in Mass Spectrometry, 31*, 2101–2108. https://doi.org/10.1002/rcm.8005

Blessing, C. H., Werner, R. A., Siegwolf, R., & Buchmann, N. (2015). Allocation dynamics of recently fixed carbon in beech saplings in response to increased temperatures and drought. *Tree Physiology, 35*, 585–598. https://doi.org/10.1093/treephys/tpv024

Bögelein, R., Thomas, F. M., & Kahmen, A. (2017). Leaf water ¹⁸O and ²H enrichment along vertical canopy profiles in a broadleaved and a conifer forest tree. *Plant, Cell & Environment, 40*, 1086–1103.

Brinkmann, N., Seeger, S., Weiler, M., Buchmann, N., Eugster, W., & Kahmen, A. (2018). Employing stable isotopes to determine the residence times of soil water and the temporal origin of water taken up by *Fagus sylvatica* and *Picea abies* in a temperate forest. *New Phytologist, 219*, 1300–1313. https://doi.org/10.1111/nph.15255

Camargo, M. A. B., & Marenco, R. A. (2011). Density, size and distribution of stomata in 35 rainforest tree species in Central Amazonia. *Acta Amazonica 41*, 205–212.

Cernusak, L. A., Barbour, M. M., Arndt, S. K., Cheesman, A. W., English, N. B., Feild, T. S., … Farquhar, G. D. (2016). Stable isotopes in leaf water of terrestrial plants. *Plant, Cell & Environment, 39*, 1087–1102.

Cernusak, L. A., Mejia-Chang, M., Winter, K., & Griffiths, H. (2008). Oxygen isotope composition of CAM and C₃ *Clusia* species: Non-steady-state dynamics control leaf water ¹⁸O enrichment in succulent leaves. *Plant, Cell & Environment, 31*, 1644–1662.

Cormier, M. A., Werner, R. A., Sauer, P. E., Gröcke, D. R., Leuenberger, M. C., Wieloch, T., … Kahmen, A. (2018). ²H-fractionations during the biosynthesis of carbohydrates and lipids imprint a metabolic signal on the δ²H values of plant organic compounds. *New Phytologist, 218*, 479–491. https://doi.org/10.1111/nph.15016

Craig, H., & Gordon, L. I. (1965). Deuterium and oxygen 18 variations in the ocean and marine atmosphere. In E. Tongiorgi (Ed.), *Proceedings of a conference on stable isotopes in oceanographic studies and paleotemperatures* (pp. 9–130). Lischi and Figli: Spoleto, Italy.

Dawson, T. E., & Goldsmith, G. R. (2018). The value of wet leaves. *New Phytologist., 219*, 1156–1169. https://doi.org/10.1111/nph.15307

Dawson, T. E., Mambelli, S., Plamboeck, A. H., Templer, P. H., & Tu, K. P. (2002). Stable isotopes in plant ecology. *Annual Review of Ecology and Systematics, 33*, 507–559.

Desalme, D., Priault, P., Gerant, D., Dannoura, M., Maillard, P., Plain, C., & Epron, D. (2017). Seasonal variations drive short-term dynamics and partitioning of recently assimilated carbon in the foliage of adult beech and pine. *New Phytologist, 213*, 140–153. https://doi.org/10.1111/nph.14124

Dongmann, G., Nurnberg, H. W., Forstel, H., & Wagener, K. (1974). Enrichment of H₂¹⁸O in leaves of transpiring plants. *Radiation and Environmental Biophysics, 11*, 41–52.

Dubbert, M., Cuntz, M., Piayda, A., & Werner, C. (2014). Oxygen isotope signatures of transpired water vapor: The role of isotopic non-steady-state transpiration under natural conditions. *New Phytologist, 203*, 1242–1252. https://doi.org/10.1111/nph.12878

Dubbert, M., Kübert, A., & Werner, C. (2017). Impact of leaf traits on temporal dynamics of transpired oxygen isotope signatures and its impact on atmospheric vapor. *Frontiers in Plant Science, 8*, 1–12.

Eller, C. B., Lima, A. L., & Oliveira, R. S. (2013). Foliar uptake of fog water and transport belowground alleviates drought effects in the cloud forest tree species, Drimys brasiliensis (Winteraceae). *New Phytologist, 199*(1), 151–162. https://doi.org/10.1111/nph.12248

Ellsworth, P. V., Ellsworth, P. Z., Anderson, W. T., & Sternberg, L. S. L. (2013). The role of effective leaf mixing length in the relationship between the d¹⁸O of stem cellulose and source water across a salinity gradient. *Plant, Cell & Environment, 36*, 138–148. https://doi.org/10.1111/j.1365-3040.2012.02562.x

Epron, D., Bahn, M., Derrien, D., Lattanzi, F. A., Pumpanen, J., Gessler, A., … Buchmann, N. (2012). Pulse-labelling trees to study carbon allocation dynamics: A review of methods, current knowledge and future prospects. *Tree Physiology, 32*, 776–798.

Farquhar, G. D., & Cernusak, L. A. (2005). On the isotopic composition of leaf water in the non-steady state. *Functional Plant Biology, 32*, 293–303.

Flanagan, L. B., Comstock, J. P., & Ehleringer, J. R. (1991). Comparison of modeled and observed environmental influences on the stable oxygen and hydrogen isotope composition of leaf water in *Phaseolus vulgaris* L. *Plant Physiology, 96*, 588–596. https://doi.org/10.1104/pp.96.2.588

Galiano Pérez, L., Timofeeva, G., Saurer, M., Siegwolf, R., Martínez-Vilalta, J., Hommel, R., & Gessler, A. (2017). The fate of recently fixed carbon after drought release: Towards unravelling C storage regulation in *Tilia platyphyllos* and *Pinus sylvestris*. *Plant, Cell & Environment, 40*, 1711–1724.

Gamarra, B., Sachse, D., & Kahmen, A. (2016). Effects of leaf water evaporative ²H-enrichment and biosynthetic fractionation on leaf wax n-alkane δ²H values in C3 and C4 grasses. *Plant, Cell & Environment, 39*, 2390–2403.

Gessler A, Brandes E, Keitel C, Boda S, Kayler ZE, Granier A, Barbour M, Farquhar GD, Treydte K. 2013. The oxygen isotope enrichment of

leaf-exported assimilates–Does it always reflect lamina leaf water enrichment? *New Phytologist* 200: 144-157.

Gessler, A., Ferrio, J. P., Hommel, R., Treydte, K., Werner, R. A., & Monson, R. K. (2014). Stable isotopes in tree rings: Towards a mechanistic understanding of isotope fractionation and mixing processes from the leaves to the wood. *Tree Physiology*, 34, 796–818. https://doi.org/10.1093/treephys/tpu040

Goldsmith, G. R. (2013). Changing directions: The atmosphere-plant-soil continuum. *New Phytologist*, 199, 4–6. https://doi.org/10.1111/nph.12332

Goldsmith, G. R., Lehmann, M. M., Cernusak, L. A., Arend, M., & Siegwolf, R. T. W. (2017). Inferring foliar water uptake using stable isotopes of water. *Oecologia*, 184, 763–766. https://doi.org/10.1007/s00442-017-3917-1

Gotsch, S. G., Asbjornsen, H., Holwerda, F., Goldsmith, G. R., Weintraub, A. E., & Dawson, T. E. (2014). Foggy days and dry nights determine crown-level water balance in a seasonal tropical montane cloud forest. *Plant, Cell & Environment*, 37, 261–272.

Helliker, B. R. (2014). Reconstructing the $\delta^{18}O$ of atmospheric water vapour via the CAM epiphyte *Tillandsia usneoides*: Seasonal controls on $\delta^{18}O$ in the field and large-scale reconstruction of $\delta^{18}O_a$. *Plant, Cell & Environment*, 37, 541–556.

Helliker, B. R., & Ehleringer, J. R. (2002a). Grass blades as tree rings: Environmentally induced changes in the oxygen isotope ratio of cellulose along the length of grass blades. *New Phytologist*, 155, 417–424.

Helliker, B. R., & Ehleringer, J. R. (2002b). Differential ^{18}O enrichment of leaf cellulose in C_3 versus C_4 grasses. *Functional Plant Biology*, 29, 435–442.

Helliker, B. R., & Griffiths, H. (2007). Toward a plant-based proxy for the isotope ratio of atmospheric water vapor. *Global Change Biology*, 13, 723–733.

Hepp, J., Tuthorn, M., Zech, R., Mugler, I., Schlutz, F., Zech, W., & Zech, M. (2015). Reconstructing lake evaporation history and the isotopic composition of precipitation by a coupled $\delta^{18}O$-δ^2H biomarker approach. *Journal of Hydrology*, 529, 622–631.

Hu, J., & Riveros-Iregui, D. A. (2016). Life in the clouds: Are tropical montane cloud forests responding to changes in climate? *Oecologia*, 180, 1061–1073. https://doi.org/10.1007/s00442-015-3533-x

Huang, L. J., & Wen, X. F. (2014). Temporal variations of atmospheric water vapor δD and $\delta^{18}O$ above an arid artificial oasis cropland in the Heihe River Basin. *Journal of Geophysical Research-Atmospheres*, 119, 11456–11476.

Kahmen, A., Sachse, D., Arndt, S. K., Tu, K. P., Farrington, H., Vitousek, P. M., & Dawson, T. E. (2011). Cellulose $\delta^{18}O$ is an index of leaf-to-air vapor pressure difference (VPD) in tropical plants. *Proceedings of the National Academy of Sciences of the United States of America*, 108, 1981–1986. https://doi.org/10.1073/pnas.1018906108

Kim, K. H., & Lee, X. H. (2011). Transition of stable isotope ratios of leaf water under simulated dew formation. *Plant, Cell & Environment*, 34, 1790–1801.

Lai, C. T., Ometto, J. P. H. B., Berry, J. A., Martinelli, L. A., Domingues, T. F., & Ehleringer, J. R. (2008). Life form-specific variations in leaf water oxygen-18 enrichment in Amazonian vegetation. *Oecologia*, 157, 197–210. https://doi.org/10.1007/s00442-008-1071-5

Lee, H., Smith, R., & Williams, J. (2006). Water vapour $^{18}O/^{16}O$ isotope ratio in surface air in New England, USA. *Tellus Series B-Chemical and Physical Meteorology*, 58, 293–304.

Lehmann, M. M., Fischer, M., Blees, J., Zech, M., Siegwolf, R. T. W., & Saurer, M. (2016). A novel methylation derivatization method for $\delta^{18}O$ analysis of individual carbohydrates by gas chromatography/pyrolysis–isotope ratio mass spectrometry. *Rapid Communications in Mass Spectrometry*, 30, 221–229. https://doi.org/10.1002/rcm.7431

Lehmann, M. M., Gamarra, B., Kahmen, A., Siegwolf, R. T. W., & Saurer, M. (2017). Oxygen isotope fractionations across individual leaf carbohydrates in grass and tree species. *Plant, Cell & Environment*, 40, 1658–1670.

Lehmann, M. M., Goldsmith, G. R., Schmid, L., Gessler, A., Saurer, M., & Siegwolf, R. T. W. (2018). The effect of ^{18}O-labelled water vapour on the oxygen isotope ratio of water and assimilates in plants at high humidity. *New Phytologist*, 217, 105–116. https://doi.org/10.1111/nph.14788

Lehmann, M. M., Rinne, K. T., Blessing, C., Siegwolf, R. T. W., Buchmann, N., & Werner, R. A. (2015). Malate as a key carbon source of leaf dark-respired CO_2 across different environmental conditions in potato plants. *Journal of Experimental Botany*, 66, 5769–5781. https://doi.org/10.1093/jxb/erv279

Liang, J., Wright, J. S., Cui, X., Sternberg, L., Gan, W., & Lin, G. (2018). Leaf anatomical traits determine the ^{18}O enrichment of leaf water in coastal halophytes. *Plant, Cell & Environment*, 41, 2744–2757. https://doi.org/10.1111/pce.13398

Mantovani, A. (1999). A method to improve leaf succulence quantification. *Brazilian Archives of Biology and Technology*, 42, 9–14.

Nadwodnik, J., & Lohaus, G. (2008). Subcellular concentrations of sugar alcohols and sugars in relation to phloem translocation in *Plantago major*, *Plantago maritima*, *Prunus persica*, and *Apium graveolens*. *Planta*, 227, 1079–1089. https://doi.org/10.1007/s00425-007-0682-0

O'Leary, M. H. (1988). Carbon isotopes in photosynthesis. *Bioscience*, 38, 328–336.

Rinne, K. T., Saurer, M., Kirdyanov, A. V., Bryukhanova, M. V., Prokushkin, A. S., Churakova, O. V., & Siegwolf, R. T. W. (2015). Examining the response of needle carbohydrates from Siberian larch trees to climate using compound-specific $\delta^{13}C$ and concentration analyses. *Plant, Cell & Environment*, 38, 2340–2352.

Rinne, K. T., Saurer, M., Streit, K., & Siegwolf, R. T. W. (2012). Evaluation of a liquid chromatography method for compound-specific d^{13}C analysis of plant carbohydrates in alkaline media. *Rapid Communications in Mass Spectrometry*, 26, 2173–2185. https://doi.org/10.1002/rcm.6334

Roden, J. S., & Ehleringer, J. R. (1999). Observations of hydrogen and oxygen isotopes in leaf water confirm the Craig-Gordon model under wide-ranging environmental conditions. *Plant Physiology*, 120, 1165–1173.

Roden, J. S., Lin, G. G., & Ehleringer, J. R. (2000). A mechanistic model for interpretation of hydrogen and oxygen isotope ratios in tree-ring cellulose. *Geochimica Et Cosmochimica Acta*, 64, 21–35.

Ruehr, N. K., Offermann, C. A., Gessler, A., Winkler, J. B., Ferrio, J. P., Buchmann, N., & Barnard, R. L. (2009). Drought effects on allocation of recent carbon: from beech leaves to soil CO_2 efflux. *New Phytologist*, 184, 950–961. https://doi.org/10.1111/j.1469-8137.2009.03044.x

Sachse, D., Billault, I., Bowen, G. J., Chikaraishi, Y., Dawson, T. E., Feakins, S. J., ... Kahmen, A. (2012). Molecular paleohydrology: Interpreting the hydrogen- isotopic composition of lipid biomarkers from photosynthesizing organisms. *Annual Review of Earth and Planetary Sciences*, 40, 221–249.

Saurer, M., Kirdyanov, A. V., Prokushkin, A. S., Rinne, K. T., & Siegwolf, R. T. W. (2016). The impact of an inverse climate–isotope relationship in soil water on the oxygen-isotope composition of *Larix gmelinii* in Siberia. *New Phytologist*, 209, 955–964. https://doi.org/10.1111/nph.13759

Schmidt, H. L., Werner, R. A., & Rossmann, A. (2001). ^{18}O pattern and biosynthesis of natural plant products. *Phytochemistry*, 58, 9–32. https://doi.org/10.1016/s0031-9422(01)00017-6

Schönbeck, L., Gessler, A., Hoch, G., McDowell, N. G., Rigling, A., Schaub, M., & Li, M.-H. (2018). Homeostatic levels of nonstructural carbohydrates after 13 yr of drought and irrigation in *Pinus sylvestris*. *New Phytologist*, 1314–1324. https://doi.org/10.1111/nph.15224

Simonin, K. A., Roddy, A. B., Link, P., Apodaca, R., Tu, K. P., Hu, J., ... Barbour, M. M. (2013). Isotopic composition of transpiration and rates of change in leaf water isotopologue storage in response to environmental variables. *Plant, Cell & Environment*, 36, 2190–2206.

Song, X., Farquhar, G. D., Gessler, A., & Barbour, M. M. (2014). Turnover time of the non-structural carbohydrate pool influences $\delta^{18}O$ of leaf cellulose. *Plant, Cell & Environment*, 37, 2500–2507.

Song, X., Simonin, K. A., Loucos, K. E., & Barbour, M. M. (2015). Modelling non-steady-state isotope enrichment of leaf water in a gas-exchange cuvette environment. *Plant, Cell & Environment*, 38, 2618–2628.

Sternberg, L. D. S. L. (2009). Oxygen stable isotope ratios of tree-ring cellulose: The next phase of understanding. *New Phytologist*, 181, 553–562.

Sternberg, L. D. S. L., DeNiro, M. J., & Savidge, R. A. (1986). Oxygen isotope exchange between metabolites and water during biochemical reactions leading to cellulose synthesis. *Plant Physiology*, 82, 423–427.

Studer, M. S., Siegwolf, R. T. W., Leuenberger, M., & Abiven, S. (2015). Multi-isotope labelling of organic matter by diffusion of $^2H/^{18}O-H_2O$ vapour and $^{13}C-CO_2$ into the leaves and its distribution within the plant. *Biogeosciences*, 12, 1865–1879.

Tremoy, G., Vimeux, F., Mayaki, S., Souley, I., Cattani, O., Risi, C., ... Oi, M. (2012). A 1-year long $\delta^{18}O$ record of water vapor in Niamey (Niger) reveals insightful atmospheric processes at different timescales. *Geophysical Research Letters*, 39, L08805. https://doi.org/10.1029/2012GL051298

Treydte, K., Boda, S., Pannatier, E. G., Fonti, P., Frank, D., Ullrich, B., ... Gessler, A. (2014). Seasonal transfer of oxygen isotopes from precipitation and soil to the tree ring: Source water versus needle water enrichment. *New Phytologist*, 202, 772–783.

Weigt, R. B., Braunlich, S., Zimmermann, L., Saurer, M., Grams, T. E., Dietrich, H. P., ... Nikolova, P. S. (2015). Comparison of $\delta^{18}O$ and $\delta^{13}C$ values between tree-ring whole wood and cellulose in five species growing under two different site conditions. *Rapid Communications in Mass Spectrometry*, 29, 2233–2244. https://doi.org/10.1002/rcm.7388

Werner, R. A. (2003). The online $^{18}O/^{16}O$ analysis: Development and application. *Isotopes in Environmental and Health Studies*, 39, 85–104. https://doi.org/10.1080/1025601031000108642

West, A. G., Patrickson, S. J., & Ehleringer, J. R. (2006). Water extraction times for plant and soil materials used in stable isotope analysis. *Rapid Communications in Mass Spectrometry*, 20, 1317–1321. https://doi.org/10.1002/rcm.2456

Yu, W., Tian, L., Ma, Y., Xu, B., & Qu, D. (2015). Simultaneous monitoring of stable oxygen isotope composition in water vapour and precipitation over the central Tibetan Plateau. *Atmospheric Chemistry and Physics*, 15, 10251–10262.

Zech, M., Tuthorn, M., Detsch, F., Rozanski, K., Zech, R., Zoller, L., ... Glaser, B. (2013). A 220 ka terrestrial $\delta^{18}O$ and deuterium excess biomarker record from an eolian permafrost paleosol sequence, NE-Siberia. *Chemical Geology*, 360, 220–230.

SUPPORTING INFORMATION

Additional supporting information may be found online in the Supporting Information section at the end of the article.

Figure S1 Linear relationships between mean residence time of O (MRT) in leaf water and assimilates and $\Delta\delta^{18}O$ values after 9 h fog exposure with a ^{18}O-depleted water vapour source ($\Delta\delta^{18}O_{Max}$) across different species. Equations of linear models and corresponding regression coefficients are given. WSC = water soluble compounds.

Figure S2 Linear relationship between $\Delta\delta^{18}O$ and $\Delta\delta^2H$ values of leaf water after 9 h fog exposure with ^{18}O- and ^2H-depleted water vapour across individual plant species of 8 different growth forms. Regression line reflects a 1:1 line.

Figure S3 Correlation matrix including isotope data (in ‰), leaf gas-exchange parameters, leaf traits and leaf sugar pool size across individual plant species of 8 different growth forms. Colors and numbers indicate the Pearson correlation coefficient. LW = $\Delta\delta^{18}O$ values of leaf water, WSC = $\Delta\delta^{18}O$ values of water soluble content, Sugars = $\Delta\delta^{18}O$ values of bulk sugars, Lth = Leaf thickness (mm); LS = Leaf succulence (kg m^{-2}); Ss and Sd = abaxial stomatal size (μm) and density (mm^{-2}); An = net assimilation rate (μmol m^{-2} s^{-1}); gs = stomatal conductance (mmol m^{-2} s^{-1}); E = transpiration rate (mmol m^{-2} s^{-1}), [Sugars] = leaf sugar pool size (% dry weight).

Figure S4 (A) Relationship between $\Delta\delta^{18}O$ of sugars ($\Delta\delta^{18}O_{Sugars}$) and $\delta^{13}C$ values after 9 h fog exposure with ^{18}O-depleted water vapour source. Photosynthetic modes (i.e. C$_3$, C$_4$, CAM) are indicated. (B) Mean $\delta^{13}C$ values of different growth forms taken before and after fog exposure. Aq = Aquatics, Co = Conifers, Ep = Epiphytes, Gr = Grasses, He = Herbs, Sh = Shrubs, Su = Succulents, Tr = Trees, AVG = average across all growth forms.

Table S1 List of plant species that have been used during the fog experiment, including their family, growth form, and plant height/length (cm), and confirmed photosynthetic mode (PM; i.e. C$_3$, C$_4$, CAM).